Journal of Cerebral Blood Flow & Metabolism (2014) 34, 1258–1269

www.jcbfm.com

FEATURE ARTICLE

The cross-talk between canonical and non-canonical Wnt-dependent pathways regulates P-glycoprotein expression in human blood–brain barrier cells

Martha L Pinzón-Daza[1,2], Iris C Salaroglio[1], Joanna Kopecka[1], Ruth Garzòn[2], Pierre-Olivier Couraud[3], Dario Ghigo[1,4] and Chiara Riganti[1,4]

In this work, we investigate if and how transducers of the 'canonical' Wnt pathway, i.e., Wnt/glycogen synthase kinase 3 (GSK3)/β-catenin, and transducers of the 'non-canonical' Wnt pathway, i.e., Wnt/RhoA/RhoA kinase (RhoAK), cooperate to control the expression of P-glycoprotein (Pgp) in blood–brain barrier (BBB) cells. By analyzing human primary brain microvascular endothelial cells constitutively activated for RhoA, silenced for RhoA or treated with the RhoAK inhibitor Y27632, we found that RhoAK phosphorylated and activated the protein tyrosine phosphatase 1B (PTP1B), which dephosphorylated tyrosine 216 of GSK3, decreasing the GSK3-mediated inhibition of β-catenin. By contrast, the inhibition of RhoA/RhoAK axis prevented the activation of PTP1B, enhanced the GSK3-induced phosphorylation and ubiquitination of β-catenin, and reduced the β-catenin-driven transcription of Pgp. The RhoAK inhibition increased the delivery of Pgp substrates like doxorubicin across the BBB and improved the doxorubicin efficacy against glioblastoma cells co-cultured under a BBB monolayer. Our data demonstrate that in human BBB cells the expression of Pgp is controlled by a cross-talk between canonical and non-canonical Wnt pathways. The disruption of this cross-talk, e.g., by inhibiting RhoAK, downregulates Pgp and increases the delivery of Pgp substrates across the BBB.

Journal of Cerebral Blood Flow & Metabolism (2014) **34,** 1258–1269; doi:10.1038/jcbfm.2014.100; published online 4 June 2014

Keywords: blood–brain barrier; β-catenin; glycogen synthase kinase 3; P-glycoprotein; RhoA kinase; Wnt

INTRODUCTION

The blood–brain barrier (BBB), a peculiar microvascular endothelium in the central nervous system, limits the delivery of drugs, xenobiotics, and toxic catabolites into the brain parenchyma, owing to the absence of fenestrations, the abundance of tight junctions and adherens junctions, and the presence of efflux transporters belonging to the ATP binding cassette family.[1] P-glycoprotein (Pgp) is one of the ATP binding cassette transporters present on the luminal side of BBB cells: it effluxes back into the bloodstream several chemotherapeutic drugs (e.g., anthracyclines, taxanes, Vinca alkaloids, epipodophyllotoxins, topotecan, methotrexate, imatinib, dasatinib, lapatinib, gefitinib, sorafenib, erlotinib), analgesics, anti-epileptics, anti-retrovirals, and antibiotics.[1]

The Wnt signaling has a central role in regulating the expression of Pgp in BBB cells[2,3] and relies on the simultaneous activation of different intracellular transducers. In the so-called 'Wnt canonical pathway', the soluble Wnt proteins bind to the Frizzled receptor and the low-density lipoprotein receptor-related protein-5 and -6 co-receptors, reduces the activity of glycogen synthase kinase 3 (GSK3), allowing the release of β-catenin from the cytosolic adenomatous polyposis coli–axin complex and its translocation into the nucleus. Here β-catenin binds to the T-cell factor/lymphoid enhancer factor and induces the transcription of target genes, such as *mdr1*, which encodes for Pgp.[4,5] We recently demonstrated that the disruption of the Wnt3 canonical pathway downregulates the Pgp expression in human BBB cells.[6]

A plethora of intracellular transducers is involved in the so-called 'non-canonical Wnt pathways'. By interacting with Frizzled, Wnt recruits Disheveled, stimulates the small GTPases RhoA and Rac, activates RhoA kinase (RhoAK), mitogen-activated protein kinase kinases, mitogen-activated protein kinases, and Jun N-terminal kinase.[4,7] By interacting with the co-receptors ROR2 and RYK, Wnt enhances the activity of phospholipase C, increases the intracellular calcium, activates protein kinase C and calmodulin kinases.[4] Wnt canonical and non-canonical pathways are often reciprocally modulated, with either cooperative or antagonistic effects.[8,9]

The Wnt non-canonical transducers RhoA and RhoAK regulate the integrity of tight junctions and the paracellular transport of substrates across BBB,[10] as well as the activity of Pgp.[11] It is not known whether Wnt/RhoA/RhoAK pathway controls also the expression of Pgp.

Aim of this work is to investigate if there are cross-talk mechanisms between the Wnt/GSK3/β-catenin canonical pathway and the Wnt/RhoA/RhoAK non-canonical pathway in human BBB

[1]Department of Oncology, School of Medicine, University of Turin, Turin, Italy; [2]Unidad de Bioquímica, Facultad de Ciencias Naturales y Matemáticas, Universidad del Rosario, Bogotá, Colombia; [3]Institut Cochin, Centre National de la Recherche Scientifique UMR 8104, Institut National de la Santé et de la Recherche Médicale (INSERM) U567, Université René Descartes, Paris, France and [4]Center for Experimental Research and Medical Studies, University of Turin, Turin, Italy. Correspondence: Professor D Ghigo, Department of Oncology, University of Turin, via Santena 5/bis, Turin 10126, Italy.
E-mail: dario.ghigo@unito.it
This work has been supported by grants from Compagnia di San Paolo, Italy (Neuroscience Program; grant 2008.1136), Italian Association for Cancer Research (AIRC; grant MFAG 11475), Italian Ministry of University and Research (Future in Research FIRB 2012 Program; grant RBFR12SOQ1) to CR. MLP-D and RG are recipients of a ERACOL Erasmus Mundus fellowship provided by EU. JK is recipient of a 'Mario and Valeria Rindi' fellowship provided by Italian Foundation for Cancer Research (FIRC).
Received 24 December 2013; revised 19 March 2014; accepted 13 April 2014; published online 4 June 2014

cells, and how these cross-talks control the expression of Pgp and the delivery of Pgp substrates across BBB.

MATERIALS AND METHODS

Chemicals

The plasticware for cell cultures was from Falcon (Becton Dickinson, Franklin Lakes, NJ, USA). Wnt activators (WntA) [2-amino-4-(3,4-(methylenedioxy)benzylamino)-6-(3-methoxyphenyl)pyrimidine] and Y27632 were purchased from Calbiochem (San Diego, CA, USA). Human recombinant Dickkopf-1 (Dkk-1) was from R&D Systems (Minneapolis, MN, USA). Rho activator II, a synthetic derivative of cytotoxic necrotizing factor from *Escherichia coli* that maintains RhoA constitutively activated,[12] was from Cytoskeleton (Denver, CO, USA). The electrophoresis reagents were obtained from Bio-Rad Laboratories (Hercules, CA, USA). The protein content of cell lysates was assessed with the BCA kit from Sigma Chemicals (St Louis, MO, USA). When not otherwise specified, all the other reagents were purchased from Sigma Chemicals.

Cells

The hCMEC/D3 cells, a primary human brain microvascular endothelial cell line that retains the BBB characteristics *in vitro*,[13] were seeded at 50,000/cm^2 density, grown for 7 days up to confluence in Petri dishes or Transwell devices (0.4 μm diameter pore size, Corning Life Sciences, Chorges, France), and cultured as previously reported.[13]

The primary human glioblastoma cells (CV17, 01010627, Nov3) were obtained from surgical samples of patients from the Neuro-Biooncology Center, Vercelli, Italy and the DIBIT San Raffaele Scientific Institute, Milan, Italy. The tumor diagnosis was performed according to WHO guidelines. The U87-MG cell line was purchased from ATCC (Manassas, VA, USA). The cells were cultured as already reported.[6] The experimental protocols were approved by the Bioethics Committee ('Comitato di Bioetica d'Ateneo'), University of Turin, Italy.

In co-culture experiments, 500,000 (for intracellular doxorubicin accumulation, cytotoxicity assays and cell cycle analysis) or 1,000 (for proliferation assay) glioblastoma cells were added in the lower chamber of Transwell devices 4 days after seeding hCMEC/D3 cells in the Transwell insert. After 3 days of co-culture, the medium of the upper chamber was replaced with fresh medium or with medium containing Y27632 and doxorubicin, alone or in combination, as detailed in the Figure legends.

Western Blot Analysis

The cells were rinsed with lysis buffer (50 mmol/L Tris, 10 mmol/L EDTA, 1% v/v Triton X-100), supplemented with the protease inhibitor cocktail set III (80 μmol/L aprotinin, 5 mmol/L bestatin, 1.5 mmol/L leupeptin, 1 mmol/L pepstatin; Calbiochem), 2 mmol/L phenylmethylsulfonyl fluoride and 1 mmol/L $NaVO_4$, then sonicated and centrifuged at 13,000 *g* for 10 minutes at 4°C. A quantity of 20 μg protein extracts were subjected to SDS–PAGE and probed with the following antibodies: anti-GSK3 (BD Biosciences, Franklin Lakes, NJ, USA); anti-phospho(Tyr216)GSK3 (BD Biosciences); anti-β-catenin (BD Biosciences); anti-phospho(Ser33/Ser37/Thr41)β-catenin (Cell Signaling Technology, Danvers, MA, USA); anti-claudin 3 (Invitrogen Life Technologies, Monza, Italy); anti-claudin 5 (Invitrogen Life Technologies); anti-occludin (Invitrogen Life Technologies); anti-zonula occludens-1 (Invitrogen Life Technologies); anti-protein tyrosine phosphatase 1B (PTP1B; Abcam, Cambridge, UK); anti-phospho(Ser50)PTP1B (Abcam); anti-Pgp (clone C219, Calbiochem); anti-multidrug resistance-related protein 1 (MRP1; Abcam); anti-breast cancer resistance protein (BCRP; Santa Cruz Biotechnology, Santa Cruz, CA, USA); anti-caspase-3 (C33, GeneTex, Hsinhu City, Taiwan); anti-β-tubulin (Santa Cruz Biotechnology), followed by a peroxidase-conjugated secondary antibody (Bio-Rad). The membranes were washed with Tris-buffered saline-Tween 0.1% v/v, and the proteins were detected by enhanced chemiluminescence (Bio-Rad).

To assess the presence of ubiquitinated β-catenin, 100 μg of proteins from whole-cell extracts were immunoprecipitated with the anti-β-catenin antibody, using the PureProteome protein A and protein G Magnetic Beads (Millipore, Billerica, MA, USA). The immunoprecipitated proteins were separated by SDS–PAGE and probed with an anti-ubiquitin antibody (Enzo Life Science, Farmingdale, NY, USA), followed by a peroxidase-conjugated secondary antibody.

A quantity of 10 μg of nuclear extracts, obtained with the Nuclear Extraction Kit (Active Motif, Rixensart, Belgium), was subjected to western blot analysis using an anti-β-catenin antibody. To check the equal control loading in nuclear fractions, the samples were probed with an anti-TATA-binding protein (TBP/TFIID) antibody (Santa Cruz Biotechnology). To exclude any cytosolic contamination of nuclear extracts, we verified that β-tubulin was undetectable in nuclear samples (not shown).

The densitometric analysis of western blots was performed with the ImageJ software (http://rsb.info.nih.gov/ij/) and expressed as arbitrary units, where '1 unit' is the mean band density of untreated hCMEC/D3 cells.

Chromatin Immunoprecipitation

The chromatin immunoprecipitation experiments were performed using the Magna ChIP A/G Chromatin Immunoprecipitation Kit (Millipore). The samples were immunoprecipitated with 5 μg of an anti-β-catenin antibody or with no antibody. The immunoprecipitated DNA was washed and eluted twice with 100 μL of elution buffer (0.1 mol/L $NaHCO_3$, 1% w/v SDS), the cross-linking was reversed by incubating the samples at 65°C for 6 hours. The samples were then treated with 1 μL proteinase K for 1 hour at 55°C. The DNA was eluted in 50 μL of H_2O and analyzed by quantitative real-time PCR (qRT–PCR). The putative β-catenin site on *mdr1* promoter was validated by the MatInspector software (http://www.genomatix.de/); the primers sequences were: 5′-CGATCCGCCTAAGAACAAAG-3′; 5′-AGCACAAA TTGAAGGAAGGAG-3′. As negative control, the immunoprecipitated samples were subjected to PCR with primers matching a region 10,000 bp upstream the *mdr1* promoter, using the following primers: 5′-GTGGTGCCTGAGGAAGAGAG-3′; 5′-GCAACAAGTAGGCACAAGCA-3′. The qRT–PCR was carried out using an IQ SYBR Green Supermix (Bio-Rad); the data were analyzed with a Bio-Rad Software Gene Expression Quantitation (Bio-Rad).

qRT–PCR

Total RNA was extracted and reverse transcribed using the QuantiTect Reverse Transcription Kit (Qiagen, Hilden, Germany). The qRT–PCR was performed with the IQ SYBR Green Supermix (Bio-Rad). The same cDNA preparation was used to quantify the genes of interest and the housekeeping gene *β-actin*. The primer sequences, designed with the Primer3 software (http://frodo.wi.mit.edu/primer3), were: for *mdr1*: 5′-TGCTGGAGC GGTTCTACG-3′; 5′-ATAGGCAATGTTCTCAGCAATG-3′; for *β-actin*: 5′- GCTAT CCAGGCTGTGCTATC-3′; 5′- TGTCACGCACGATTTCC-3′. The relative quantification was performed by comparing each PCR product with the housekeeping PCR product, using the Bio-Rad Software Gene Expression Quantitation (Bio-Rad).

RhoA and RhoA Kinase Activity

To evaluate the RhoA activity, the RhoA-GTP-bound fraction, taken as an index of monomeric G-proteins activation,[11] was measured using the G-LISA RhoA Activation Assay Biochem Kit (Cytoskeleton), according to the manufacturer's instructions. The absorbance was read at 450 nm, using a Packard EL340 microplate reader (Bio-Tek Instruments, Winooski, VT, USA). For each set of experiments, a titration curve was prepared, using serial dilutions of the Rho-GTP positive control of the kit. The data were expressed as U absorbance/mg cell proteins. The RhoAK activity was measured using the CycLex Rho Kinase Assay Kit (CycLex, Nagano, Japan), following the manufacturer's instructions. For each set of experiments, a titration curve was set, using serial dilutions of recombinant RhoAK (MBL, Woburn, MA, USA). The data were expressed as U absorbance/mg cell proteins.

RhoA Small Interfering RNA Transfection

A quantity of 200,000 cells were transfected with 400 nmol/L of 20 to 25 nucleotide non-targeting scrambled small interfering RNAs (Control siRNA-A, Santa Cruz Biotechnology) or specific RhoA siRNAs (Santa Cruz Biotechnology), as reported previously.[14] To verify the silencing efficacy, 48 hours after the transfection, the cells were lysed and checked for the expression of RhoA by western blotting, using an anti-RhoA antibody (Santa Cruz Biotechnology).

Protein Tyrosine Phosphatase 1B Activity

To measure the activity of endogenous PTB1B in cell lysates, the PTP1B Inhibitor Screening Assay kit (Abcam) was used. Cells untreated or treated with RhoA activator II, Y27632 or both, were washed twice in ice-cold PBS, detached by trypsin/EDTA, rinsed with 0.5 mL of PTP1B assay buffer provided by the kit and sonicated. Cell lysate (200 μL), each containing

100 μg proteins, were transferred into a 96-wells plate, in the presence of 100 μmol/L PTP1B substrate from the kit. The plates were incubated for 30 minutes at 37°C, then 100 μL of the Red Assay reagent of the kit was added for 20 minutes. The absorbance at 620 nm was read using a Packard EL340 microplate reader.

The activity of purified PTP1B was measured in a cell-free system: 5 U of human recombinant PTP1B protein (Abcam), diluted in 100 μL of reaction buffer (10 mmol/L Tris/HCl, 50 mmol/L NaCl, 2 mmol/L dithiothreitol, 1 mmol/L $MnCl_2$; pH 7.5), was incubated for 10 minutes at 37°C, with 10 μg of a recombinant peptide from human GSK3 containing phosphorylated tyrosine 216 (Abcam). To test if RhoAK affects the dephosphorylation of GSK3 by PTP1B, in a parallel set of experiments, PTP1B protein was preincubated for 30 minutes at 37°C with 10 U of human recombinant RhoAK (MBL), diluted in 100 μL of the Rho Kinase buffer (from CycLex Rho Kinase Assay Kit) containing 25 mmol/L ATP. When indicated, 10 μmol/L of the RhoAK inhibitor Y27632 was added. After this preincubation step, a 10 μL aliquot from each sample was removed and used to measure the phosphorylation of PTP1B on serine 50 by western blot analysis. The remaining sample was incubated for 10 minutes at 37°C with the phospho(Tyr 216)-GSK3 peptide, as reported above. In all samples, the reaction was stopped by adding 100 μL of the Red Assay reagent from the PTP1B Inhibitor Screening Assay kit; the absorbance at 620 nm was read after 20 minutes. For each set of experiments, a titration curve was prepared, using serial dilutions of the phosphate standard from the PTP1B Inhibitor Screening Assay kit. Data were expressed as nmol phosphate/mL. The activity of endogenous PTP1B was then expressed as percentage of the activity of PTP1B of each sample versus the activity of PTP1B measured in untreated cells. The activity of purified PTP1B was expressed as percentage of the activity of PTP1B measured after the preincubation step with RhoAK versus the activity of PTP1B measured without the preincubation step with RhoAK.

Permeability Assays Across Blood–Brain Barrier

The permeability to dextran–fluorescein isothiocyanate (molecular weight 70 kDa), [^{14}C]-sucrose (molecular weight: 342.30 Da; 589 mCi/mmol; PerkinElmer, Waltham, MA, USA), [^{14}C]-inulin (molecular weight range: 5.0 to 5.5 kDa; 10 mCi/mmol; PerkinElmer), sodium fluorescein (molecular weight: 376.27 Da) was taken as a parameter of tight junction integrity[11,15] and measured as previously reported.[6,16]

To measure the permeability coefficient of doxorubicin across the BBB monolayer, wild-type or RhoA-silenced hCMEC/D3 cells were grown for 7 days up to confluence in 6-multiwell Transwell devices, and treated as reported under the Results section. Doxorubicin (5 μmol/L) was added in the upper Transwell chamber for 3 hours, then the medium in the lower chamber was collected and the amount of doxorubicin was measured fluorimetrically, using an LS-5 Spectrofluorimeter (PerkinElmer). The excitation and emission wavelengths were 475 nm and 553 nm, respectively. The fluorescence was converted in nmol doxorubicin/cm^2, using a calibration curve prepared previously. The permeability coefficients were calculated as reported earlier.[17]

Intratumor Doxorubicin Accumulation in Co-Culture Models

After 3 days of co-culture, doxorubicin (5 μmol/L for 3 hours) or Y27632 (10 μmol/L for 3 hours) followed by doxorubicin (5 μmol/L for 3 hours) were added to the upper chamber of a Transwell insert containing an hCMEC/D3 cell monolayer. Then glioblastoma cells were collected from the lower chamber, rinsed with PBS, re-suspended in 0.5 mL ethanol/HCl 0.3 N (1:1 v/v) and sonicated. A 50 μL aliquot was used to measure the protein content; the remaining sample was used to quantify fluorimetrically the intracellular doxorubicin content, as described above. The results were expressed as nmol doxorubicin/mg cell proteins.

For fluorescence microscope analysis, the glioblastoma cells in the lower chamber were seeded on sterile glass coverslips and treated as reported above. At the end of the incubation period, the cells were rinsed with PBS, fixed in 4% w/v paraformaldehyde for 15 minutes, washed three times with PBS and incubated with 4′,6-diamidino-2-phenylindole dihydrochloride for 3 minutes at room temperature in the dark. The cells were washed three times with PBS and once with water, then the slides were mounted with 4 μL of Gel Mount Aqueous Mounting and examined with a Leica DC100 fluorescence microscope (Leica Microsystems, Wetzlar, Germany). For each experimental point, a minimum of five microscopic fields were examined.

Cytotoxicity, Cell Cycle Analysis and Cell Proliferation of Glioblastoma Cells in Co-Culture Models

For cytotoxicity, apoptosis, and cell cycle analysis, after 3 days of co-culture, doxorubicin (5 μmol/L for 24 hours) or Y27632 (10 μmol/L for 3 hours) followed by doxorubicin (5 μmol/L for 24 hours) were added to the upper chamber of Transwell inserts containing an hCMEC/D3 cell monolayer.

The release of lactate dehydrogenase in the supernatant of glioblastoma cells, used as an index of cell damage and necrosis, was measured spectrophotometrically as described earlier.[18] The apoptosis of glioblastoma cells was assessed by analyzing the cleavage of caspase-3 by western blotting, as described above. For cell cycle distribution, the glioblastoma cells were washed twice with fresh PBS, incubated in 0.5 mL of ice-cold 70% v/v ethanol for 15 minutes, then centrifuged at 1,200 *g* for 5 minutes at 4°C and rinsed with 0.3 mL of citrate buffer (50 mmol/L Na_2HPO_4, 25 mmol/L sodium citrate, 1% v/v Triton X-100), containing 10 μg/mL propidium iodide and 1 mg/mL RNAse (from bovine pancreas). After 15-minute incubation in the dark, the intracellular fluorescence was detected by a FACSCalibur flow cytometer (Becton Dickinson). For each analysis, 10,000 events were collected and analyzed by the Cell Quest software (Becton Dickinson).

To monitor the long-term cell proliferation, 1,000 glioblastoma cells were seeded in the lower chamber of Transwell, containing confluent hCMEC/D3 cells in the insert. This time was considered 'day 0' in the proliferation assay. After 3 days of co-culture, the upper chamber of the Transwell insert was filled with fresh medium or medium containing 10 μmol/L Y27632 for 3 hours, 5 μmol/L doxorubicin for 24 hours, 10 μmol/L Y27632 for 3 hours followed by 5 μmol/L doxorubicin for 24 hours. The treatments were repeated every 7 days, for 4 weeks. At day 7, 14, 21, and 28 the glioblastoma cells were collected, transferred into a 96-wells plate, fixed with 4% w/v paraformaldehyde and stained with 0.5% w/v crystal violet solution for 10 minutes at room temperature. The plate was washed three times in water, then 100 μL of 0.1 mmol/L sodium citrate in 50% v/v ethanol was added to each well and the absorbance was read at 570 nm. The absorbance units were converted into the number of cells, according to a titration curve obtained with serial cell dilutions of each cell line. To check if the hCMEC/D3 cells retained BBB properties, the permeability to dextran and inulin was measured weekly in a parallel set of Transwell. No significant changes in the permeability coefficients were detected during the whole experiment (not shown).

Pgp ATPase Assay

The rate of ATP hydrolysis was measured spectrophotometrically on Pgp immunoprecipitated from the membrane of hCMEC/D3 cells as described previously.[11]

Statistical Analysis

All data in the text and figures are provided as means ± s.d. The results were analyzed by a one-way analysis of variance. A $P < 0.05$ was considered significant.

RESULTS

Wnt Controls the GSK3/β-Catenin and RhoA/RhoA Kinase Activities in Human Blood–Brain Barrier Cells

The hCMEC/D3 cells exhibited a GSK3 constitutively phosphorylated on tyrosine 216, i.e., activated, and a β-catenin constitutively phosphorylated on serine 33, serine 37 and threonine 41 (Figure 1A), i.e., primed for ubiquitination. Notwithstanding, we detected in the untreated hCMEC/D3 cells a basal amount of β-catenin translocated into the nucleus (Figure 1B) and bound to the promoter of *mdr1* gene (Figure 1C), which encodes for Pgp. In line with previous findings obtained on hCMEC/D3 cells and primary human brain microvascular endothelial cells,[6] the Wnt activator WntA decreased the phosphorylation/activation of GSK3, strongly reduced the phosphorylation of β-catenin (Figure 1A), increased the nuclear translocation and the binding of β-catenin to the *mdr1* promoter (Figures 1B and 1C); the Wnt inhibitor Dkk-1 produced opposite effects (Figures 1A–C). In keeping with these results, WntA increased and Dkk-1 decreased the mRNA level of *mdr1* in hCMEC/D3 cells (Figure 1D). In parallel, Wnt modulated

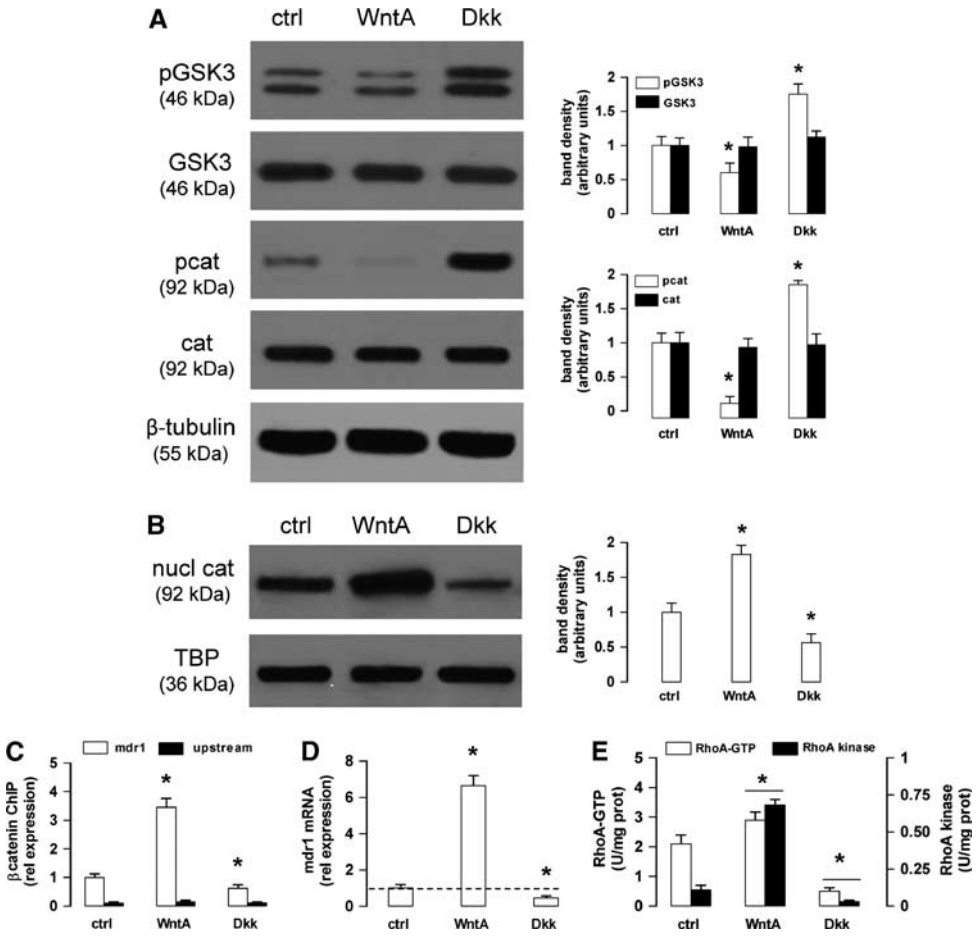

Figure 1. Wnt controls the β-catenin-induced transcription of P-glycoprotein (Pgp) and RhoA activity in human blood–brain barrier cells. The hCMEC/D3 cells were grown in fresh medium (ctrl), with the Wnt activator 2-amino-4-(3,4-(methylenedioxy)benzylamino)-6-(3-methoxyphenyl)pyrimidine (WntA; 20 μmol/L for 24 hours) or the Wnt inhibitor Dickkopf-1 (Dkk-1) protein (Dkk; 1 μg/mL for 24 hours). (**A**) Western blot analysis of phospho(Tyr216)GSK3 (glycogen synthase kinase 3) (pGSK3), GSK3, phospho(Ser33/Ser37/Thr41)β-catenin (pcat), β-catenin (cat) in whole-cell lysates. The β-tubulin expression was used as a control of equal protein loading. The figure is representative of three experiments with similar results. The band density ratio between each protein and β-tubulin was expressed as arbitrary units. Versus ctrl cells: $^*P<0.02$. (**B**) Nuclear extracts were analyzed for the amount of β-catenin (nucl cat). The expression of TATA-binding protein (TBP) was used as a control of equal protein loading. The figure is representative of three experiments with similar results. The band density ratio between each protein and TBP was expressed as arbitrary units. Versus ctrl cells: $^*P<0.02$. (**C**) Chromatin Immunoprecipitation assay. The genomic DNA was extracted, immunoprecipitated with an anti-β-catenin antibody and analyzed by quantitative real-time PCR (qRT–PCR), using primers for the β-catenin binding site on mdr1 promoter (open bars) or for an upstream region (black bars), chosen as a negative control. Results are presented as means ± s.d. ($n=4$). Versus ctrl: $^*P<0.05$. (**D**) The mdr1 expression was detected by qRT–PCR. Data are presented as means ± s.d. ($n=4$). Versus ctrl: $^*P<0.02$. (**E**) RhoA/RhoA kinase (RhoAK) activity. The samples were subjected to enzyme-linked immunosorbent assays to measure the amount of RhoA-GTP (open bars) and the activity of RhoAK (black bars). Data are presented as means ± s.d. ($n=4$). Versus ctrl: $^*P<0.05$.

the activity of RhoA and RhoAK: as shown in Figure 1E, WntA increased and Dkk-1 decreased the GTP binding to RhoA and the activity of RhoAK. These data suggest that both Wnt/GSK3 canonical pathway and Wnt/RhoA/RhoAK non-canonical pathway are active in the hCMEC/D3 cells and vary their activity in response to Wnt activators and inhibitors at the same time.

RhoA Modulates the GSK3/β-Catenin-Driven Transcription of Pgp in Human Blood–Brain Barrier Cells

To investigate whether the activity of non-canonical Wnt/RhoA/RhoAK pathway controls the activity of canonical Wnt/GSK3 pathway in hCMEC/D3 cells, we constitutively activated RhoA with the RhoA activator II[12] (Figure 2A) and silenced RhoA (Figure 2B), respectively. The cells with active RhoA showed a reduced phosphorylation of GSK3 and β-catenin (Figure 2C), and an increased β-catenin nuclear translocation (Figure 2D). By contrast, the RhoA-silenced cells exhibited a higher amount of phosphorylated GSK3 and β-catenin (Figure 2C), and a reduced β-catenin nuclear translocation (Figure 2D). These data suggest that the activity of the Wnt non-canonical transducer RhoA controls the activation of the Wnt canonical transducers GSK3/β-catenin in our model.

Of note for the aim of this work, the RhoA activation increased, while the RhoA silencing decreased the binding of β-catenin to *mdr1* promoter (Figure 2E) and the levels of *mdr1* mRNA (Figure 2F) in the hCMEC/D3 cells. The increase of *mdr1* expression induced by WntA or RhoA activator II was not paralleled by an increase in permeability to small molecules, such as sucrose and sodium fluorescein (Supplementary Figure 1), thus ruling out a Wnt- or RhoA-mediated increase of the monolayer passive permeability.

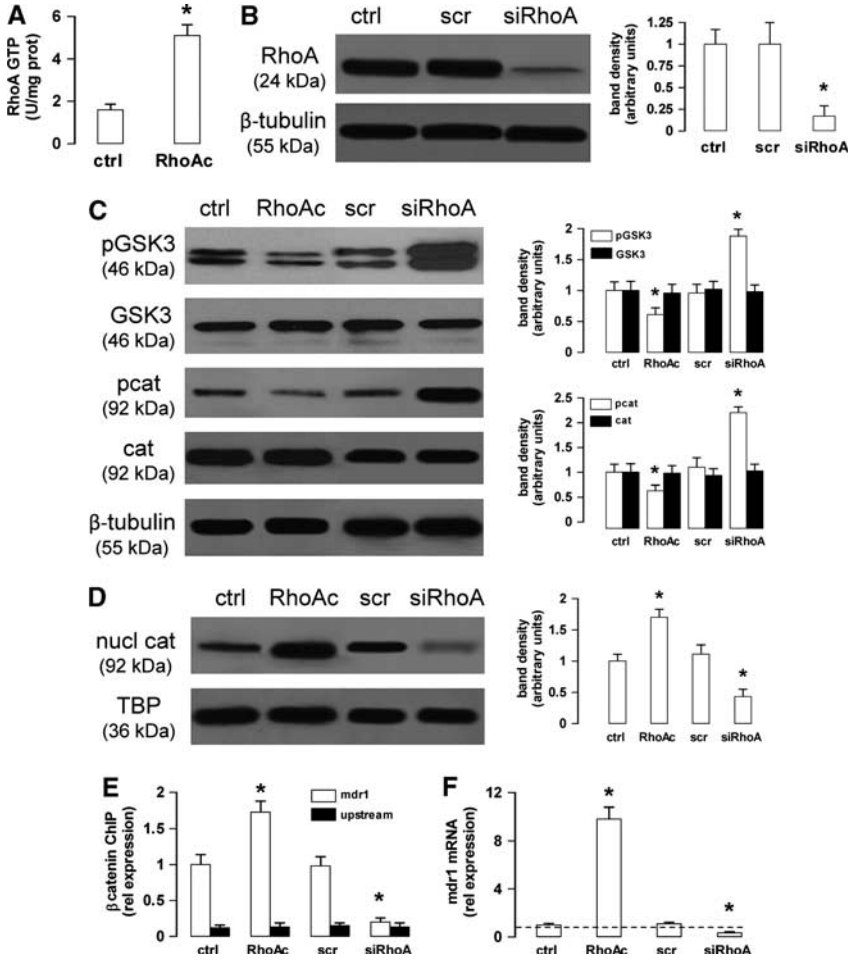

Figure 2. The RhoA activity controls the glycogen synthase kinase 3 (GSK3)/β-catenin-driven transcription of P-glycoprotein (Pgp) in human blood–brain barrier cells. (**A**) The hCMEC/D3 cells were grown in fresh medium in the absence (ctrl) or in the presence of the RhoA activator II (RhoAc; 5 μg/mL for 3 hours), then the activity of RhoA was measured by an enzyme-linked immunosorbent assay. Data are presented as means ± s.d. ($n = 4$). Versus ctrl: *$P < 0.005$. (**B**) The cells were cultured for 48 hours with fresh medium (ctrl), treated with a non-targeting scrambled small interfering RNA (siRNA) (scr) or a RhoA-targeting specific siRNA pool (siRhoA). The expression of RhoA was measured in whole-cell lysates by western blotting. The β-tubulin expression was used as a control of equal protein loading. The figure is representative of three experiments with similar results. The band density ratio between each protein and β-tubulin was expressed as arbitrary units. Versus ctrl cells: *$P < 0.005$. (**C**) Western blot analysis of phospho(Tyr216)GSK3 (pGSK3), GSK3, phospho(Ser33/Ser37/Thr41)β-catenin (pcat), β-catenin (cat) in whole-cell lysates of hCMEC/D3 cells treated as described in (**A** and **B**). The β-tubulin expression was used as a control of equal protein loading. The figure is representative of three experiments with similar results. The band density ratio between each protein and β-tubulin was expressed as arbitrary units. Versus ctrl cells: *$P < 0.05$. (**D**) Nuclear extracts from cells treated as described in (**A** and **B**) were analyzed for the amount of β-catenin (nucl cat). The expression of TATA-binding protein (TBP) was used as a control of equal protein loading. The band density ratio between each protein and TBP was expressed as arbitrary units. Versus ctrl cells: *$P < 0.005$. (**E**) Cells were cultured as reported in (**A** and **B**). After 3 hours (for the RhoAc II-treated cells) or 48 hours (for the scrambled- and RhoA-targeting siRNA-treated cells), the genomic DNA was extracted, immunoprecipitated with an anti-β-catenin antibody and analyzed by quantitative real-time PCR (qRT–PCR), using primers for the β-catenin binding site on the mdr1 promoter (open bars) or for an upstream region (black bars), chosen as a negative control. The ctrl bars in the figure correspond to the DNA extracted after 48 hours from hCMEC/D3 cells; the results were superimposable for the DNA extracted after 3 hours (not shown in the figure). Results are expressed as means ± s.d. ($n = 4$). Versus ctrl: *$P < 0.01$. (**F**) The cells were treated as detailed in (**A** and **B**). After 3 hours (for the RhoAc II-treated cells) or 48 hours (for the scrambled- and RhoA-targeting siRNA-treated cells), the mdr1 expression was detected by qRT–PCR. Data are presented as means ± s.d. ($n = 4$). Versus ctrl *$P < 0.005$.

The RhoA Kinase Inhibition Reduces the Pgp Transcription in Blood–Brain Barreir Cells, by Inhibiting the Protein Tyrosine Phosphatase 1B Activity and Increasing the Glycogen Synthase Kinase 3-Mediated Phosphorylation and Ubiquitination of β-Catenin

As in hCMEC/D3 cells, Wnt controls the activity of RhoA and its downstream effector RhoAK (Figure 1E), we next investigated whether RhoAK mediated the cross-talk between the Wnt/GSK3 canonical pathway and the Wnt/RhoA non-canonical pathway. Time-dependence experiments with the RhoAK inhibitor Y27632 showed that at 10 μmol/L, this compound effectively inhibited the RhoAK activity at each time point considered (Supplementary Figure 2A) and decreased the β-catenin nuclear translocation at the time points from 3 to 24 hours (Supplementary Figure 2B). After 3 hours, when the reduction of RhoAK activity and β-catenin was maximal, Y27632 did not change the expression of claudin-3, claudin-5, occludin, zonula occludens-1 (Supplementary Figure 2C) and did not alter the permeability coefficient of dextran, inulin and sucrose (Supplementary Figure 2D), suggesting that the RhoAK inhibition did not affect the integrity of tight junctions and

the paracellular transport processes. In the light of these results, Y27632 was used at 10 μmol/L for 3 hours in all the following experiments: in these conditions, Y27632 increased the phosphorylation of GSK3 and β-catenin (Figure 3A) and reduced the β-catenin nuclear translocation (Figure 3B), also in the presence of a constitutively activated RhoA (Figures 3A and 3B).

The tyrosine phosphatase PTP1B reduces the activity of GSK3 by dephosphorylating tyrosine 216, which is critical for the GSK3 activity.[19] PTP1B is in its turn activated by the phosphorylation on serine 50, operated by serine/threonine kinases.[20] We thus wondered whether RhoAK may modulate the GSK3 phosphorylation via PTP1B.

PTP1B was basally phosphorylated on serine 50 in the hCMEC/D3 cells (Figure 3C). Interestingly, the cells with activated RhoA had increased levels of phospho(Ser50)PTP1B, which was strongly reduced in cells treated with the RhoAK inhibitor Y27632. The latter also abolished the phosphorylation of PTP1B induced by active RhoA (Figure 3C). The endogenous activity of PTP1B was significantly increased in cells with activated RhoA and significantly decreased in Y27632-treated cells (Figure 3D). To test whether RhoAK, by phosphorylating PTP1B on serine 50, may decrease the phosphorylation of GSK3 on tyrosine 216, we set up a cell-free system and measured the activity of recombinant PTP1B protein, using as a substrate a synthetic peptide derived from GSK3, containing the phosphorylated tyrosine 216 (Figures 3E and 3F). PTP1B, when preincubated with the recombinant RhoAK in this cell-free system, was phosphorylated on serine 50, an effect that was prevented by Y27632 (Figure 3E). In keeping with this observation, the preincubation with RhoAK increased the PTP1B-mediated dephosphorylation of the recombinant phospho(Tyr 216)GSK3 peptide; such a dephosphorylation was significantly reduced by the RhoAK inhibitor Y27632 (Figure 3F).

These data suggest that RhoAK activates PTP1B, promotes the tyrosine dephosphorylation of GSK3 and its inhibition, whereas the RhoAK inhibition produces opposite effects.

As an active GSK3 promotes the phosphorylation of β-catenin, priming it for the subsequent ubiquitination and proteasomal degradation,[4,5] we next measured the β-catenin ubiquitination in the presence of RhoA/RhoAK activators or inhibitors. The untreated hCMEC/D3 cells showed a basal level of β-catenin ubiquitination (Figure 4A), which was in line with the basal phosphorylation of the protein on serine 33, serine 37, and threonine 41 (Figure 1A). The ubiquitination of β-catenin was reduced in cells with active RhoA and increased by the RhoA silencing or the RhoAK inhibitor Y27632 (Figure 4A). These data suggest that an active RhoAK prevents the ubiquitination of β-catenin and highlight the possibility to regulate the transcription of β-catenin-target genes by modulating the RhoAK activity. As the silencing of RhoA did (Figures 2E and 2F), also Y27632 decreased the binding of β-catenin to the *mdr1* promoter (Figure 4B) and the levels of *mdr1* mRNA (Figure 4C). Both RhoA silencing and RhoAK inhibition reduced the Pgp protein levels, whereas RhoA increased them; by contrast, these treatments did not change the amount of MRP1 and BCRP, two other ATP binding cassette transporters present on the luminal side of BBB cells[1] (Figure 4D).

To verify whether the inhibition of RhoA and RhoAK increases the delivery of Pgp substrates across the BBB, we used doxorubicin,[21] which exhibited a low permeability across the hCMEC/D3 cell monolayer (Figure 4E), owing to the high level of Pgp on the luminal side of these cells.[22] The doxorubicin permeability was further decreased by active RhoA, but it was increased by RhoA silencing or Y27632 (Figure 4E). The latter, which counteracted the effect of RhoA activator II on β-catenin ubiquitination (Figure 4A), also prevented the effects of RhoA activation on β-catenin binding to *mdr1* promoter (Figure 4B), *mdr1* transcription (Figure 4C), Pgp protein levels (Figure 4D) and doxorubicin permeability (Figure 4E).

The Inhibition of RhoA Kinase Increases the Doxorubicin Delivery and Cytotoxicity in Human Glioblastoma Cells Co-Cultured with Blood–Brain Barrier Cells

As the inhibition of RhoAK increased the doxorubicin permeability across the hCMEC/D3 monolayer, we wondered whether priming the BBB cells with Y27632 improves the delivery of doxorubicin to glioblastoma cells grown under the BBB monolayer.

The doxorubicin accumulation within glioblastoma cells (CV17, 01010627, Nov3 and U87-MG) co-cultured with hCMEC/D3 cells was low, as evaluated by fluorimetric assays (Figure 5A) and fluorescence microscope analysis (Figure 5B). The pretreatment of the hCMEC/D3 cells with Y27632 significantly increased the doxorubicin retention within glioblastoma cells (Figures 5A and 5B). Doxorubicin alone did not produce significant cell damages in terms of release of lactate dehydrogenase in the extracellular medium of glioblastoma cells (Figure 5C), and induced weak signs of apoptosis, as suggested by the low level of cleaved caspase-3 (Figure 5D). When effective, the drug is expected to induce a G2/M-phase arrest, which was not observed in the 01010627 glioblastoma cells co-cultured under the hCMEC/D3 monolayer exposed to doxorubicin alone (Figure 5E). The exposure to Y27632 followed by doxorubicin strongly increased the release of lactate dehydrogenase (Figure 5C), the cleavage of caspase-3 (Figure 5D), the percentage of cells arrested in G2/M phase (Figure 5E). In parallel, such combination increased the amount of cells in pre-G1 phase, an index of apoptotic cells, and decreased the number of cells in S phase (Figure 5E). Of note, used at 10 μmol/L for 3 hours, Y27632 alone was not cytotoxic for glioblastoma cells (Figures 5C–E). The repeated administration of Y27632 or doxorubicin as single agents on the luminal side of the hCMEC/D3 monolayer did not reduce the proliferation of 01010627 glioblastoma cells growing under this model of BBB (Figure 5F); only the pretreatment of hCMEC/D3 cells with Y27632 followed by doxorubicin significantly decreased the long-term proliferation of tumor cells (Figure 5F).

Interestingly, the pretreatment with Y27632 produced the same effects of verapamil, a strong inhibitor of Pgp activity in the hCMEC/D3 cells (Supplementary Figure 3A); when co-incubated with doxorubicin, verapamil increased the drug permeability across the BBB monolayer (Supplementary Figure 3B) and its accumulation in co-cultured glioblastoma cells (Supplementary Figure 3C), as well as lactate dehydrogenase release (Supplementary Figure 3D), caspase-3 activation (Supplementary Figure 3E), G2/M-arrest (Supplementary Figure 3F) in glioblastoma cells.

DISCUSSION

In this work, we demonstrate that the expression of Pgp in human BBB cells is controlled by a cross-talk between the Wnt/GSK3 canonical pathway and the Wnt/RhoA/RhoAK non-canonical pathway. The activation of Wnt/GSK3/β-catenin axis is known to increase the expression of Pgp in hCMEC/D3 cells.[2,3,6] The activation of RhoA and RhoAK is known to enhance the Pgp activity in BBB cells.[11] It is not known: (1) whether the Wnt/RhoA/RhoAK axis controls also the Pgp expression; (2) whether the canonical and non-canonical Wnt pathways cooperate in regulating the Pgp levels in BBB cells.

We observed that the Wnt activation increases at the same time the activity of GSK3 and the activity of RhoA/RhoAK in hCMEC/D3 cells, while the Wnt inhibition reduces them. The positive cooperation between Wnt/GSK3 and Wnt/RhoA/RhoAK axis, which we detected in BBB cells, has been described in pulmonary aortic endothelial cells: here the bone morphogenetic protein 2 increases the activity of GSK3/β-catenin axis and at the same time recruits the Wnt-downstream effector Disheveled, which activates RhoA.[23] As WntA activates Disheveled, and Dkk-1 inhibits it in most mammalian cells,[4] it is likely that also in our model the changes in RhoA/RhoAK activity in response to WntA and Dkk-1 were due to the changes in Disheveled activity.

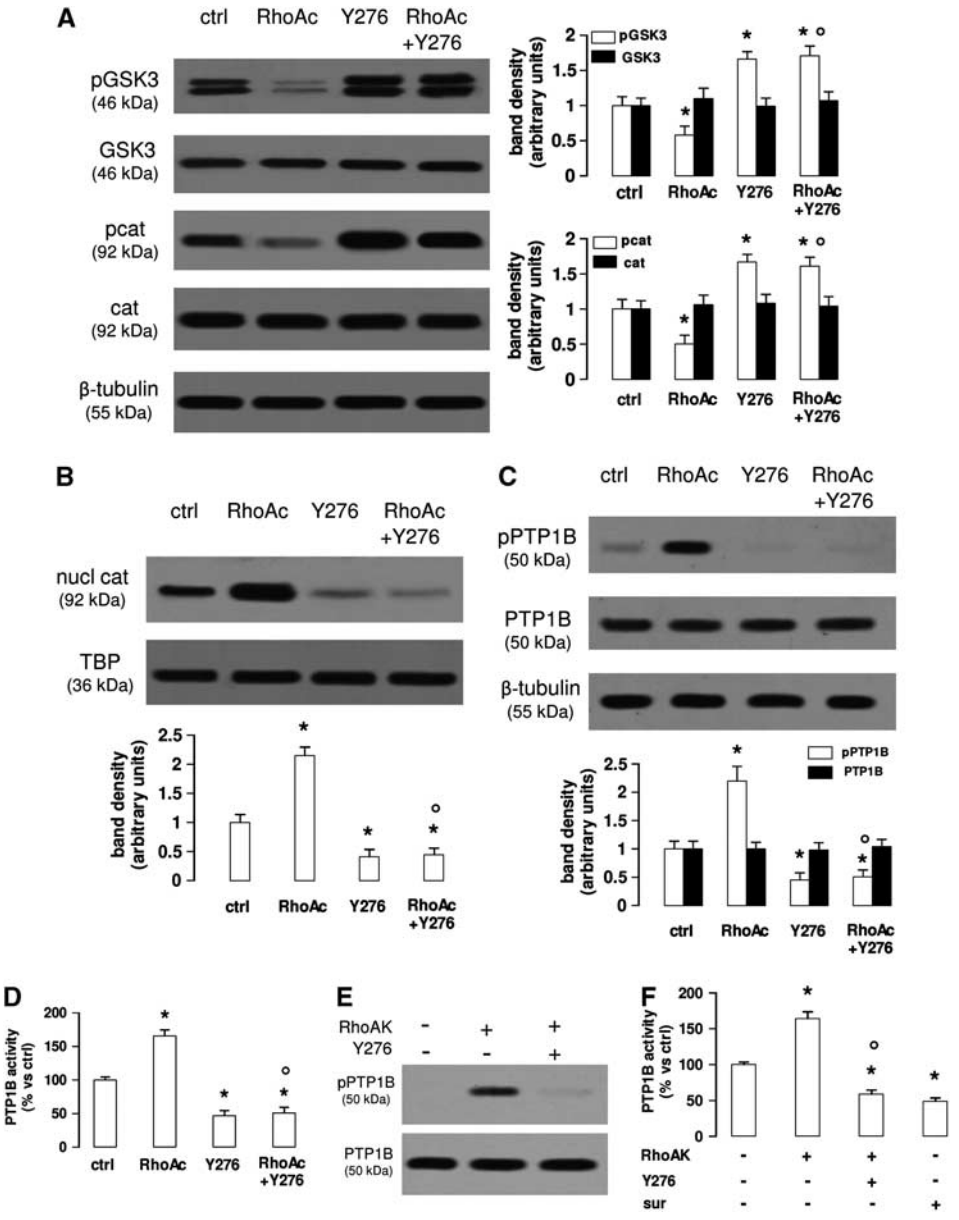

Figure 3. The RhoA kinase (RhoAK) inhibition increases the activation of glycogen synthase kinase 3 (GSK3), by decreasing the activity of protein tyrosine phosphatase 1B (PTP1B) in human blood–brain barrier cells. The hCMEC/D3 cells were grown in fresh medium (ctrl) or in medium containing the RhoA activator II (RhoAc; 5 μg/mL for 3 hours) or the RhoAK inhibitor Y27632 (*Y276*; 10 μmol/L for 3 hours), alone or co-incubated. (**A**) Western blot analysis of phospho(Tyr216)GSK3 (pGSK3), GSK3, phospho(Ser33/Ser37/Thr41)β-catenin (pcat), β-catenin (cat) in whole-cell lysates. The β-tubulin expression was used as a control of equal protein loading. The figure is representative of three experiments with similar results. The band density ratio between each protein and β-tubulin was expressed as arbitrary units. Versus ctrl cells: $^*P<0.05$; versus RhoAc alone: $^\circ P<0.001$. (**B**) The nuclear extracts were analyzed for the amount of β-catenin (nucl cat). The expression of TATA-binding protein (TBP) was used as a control of equal protein loading. The band density ratio between each protein and TBP was expressed as arbitrary units. Versus ctrl cells: $^*P<0.002$; versus RhoAc alone: $^\circ P<0.001$. (**C**) Western blot analysis of phospho(Ser50)PTP1B (pPTP1B) and PTP1B. The β-tubulin expression was used as a control of equal protein loading. The figure is representative of three experiments with similar results. The band density ratio between each protein and β-tubulin was expressed as arbitrary units. Versus ctrl cells: $^*P<0.005$; versus RhoAc alone: $^\circ P<0.001$. (**D**) The activity of endogenous PTP1B was measured in cell lysates, as reported under Materials and Methods. Data are presented as means ± s.d. ($n=3$). Versus ctrl: $^*P<0.002$; versus RhoAc alone: $^\circ P<0.001$. (**E**) *In vitro* phosphorylation of PTP1B in the presence of RhoAK and Y27632. 5 U of human recombinant PTP1B were incubated in the absence (−) or in the presence of 10 U of human recombinant RhoAK, alone or in the presence of the RhoAK inhibitor Y27632 (*Y276*; 10 μmol/L) for 30 minutes at 37°C, in a reaction buffer containing 25 mmol/L ATP. At the end of this incubation time, samples were resolved by SDS–PAGE and probed with anti-phospho(Ser50)PTP1B (pPTP1B) or anti-PTP1B antibodies. The figure is representative of three experiments with similar results. (**F**) The activity of purified PTP1B was measured in a cell-free system, using a recombinant phospho(Tyr 216)GSK3 peptide as substrate. When indicated, 10 U of RhoAK, alone or in the presence of Y27632 (*Y276*; 10 μmol/L), were added in the reaction mix 30 minutes before adding the phospho(Tyr 216)GSK3 peptide. Suramin (sur; 10 μmol/L), a known inhibitor of PTP1B, was added together with the phospho(Tyr 216)GSK3 peptide, as internal control. Data are presented as means ± s.d. ($n=3$). Versus PTP1B alone (−): $^*P<0.002$; versus RhoAK: $^\circ P<0.001$.

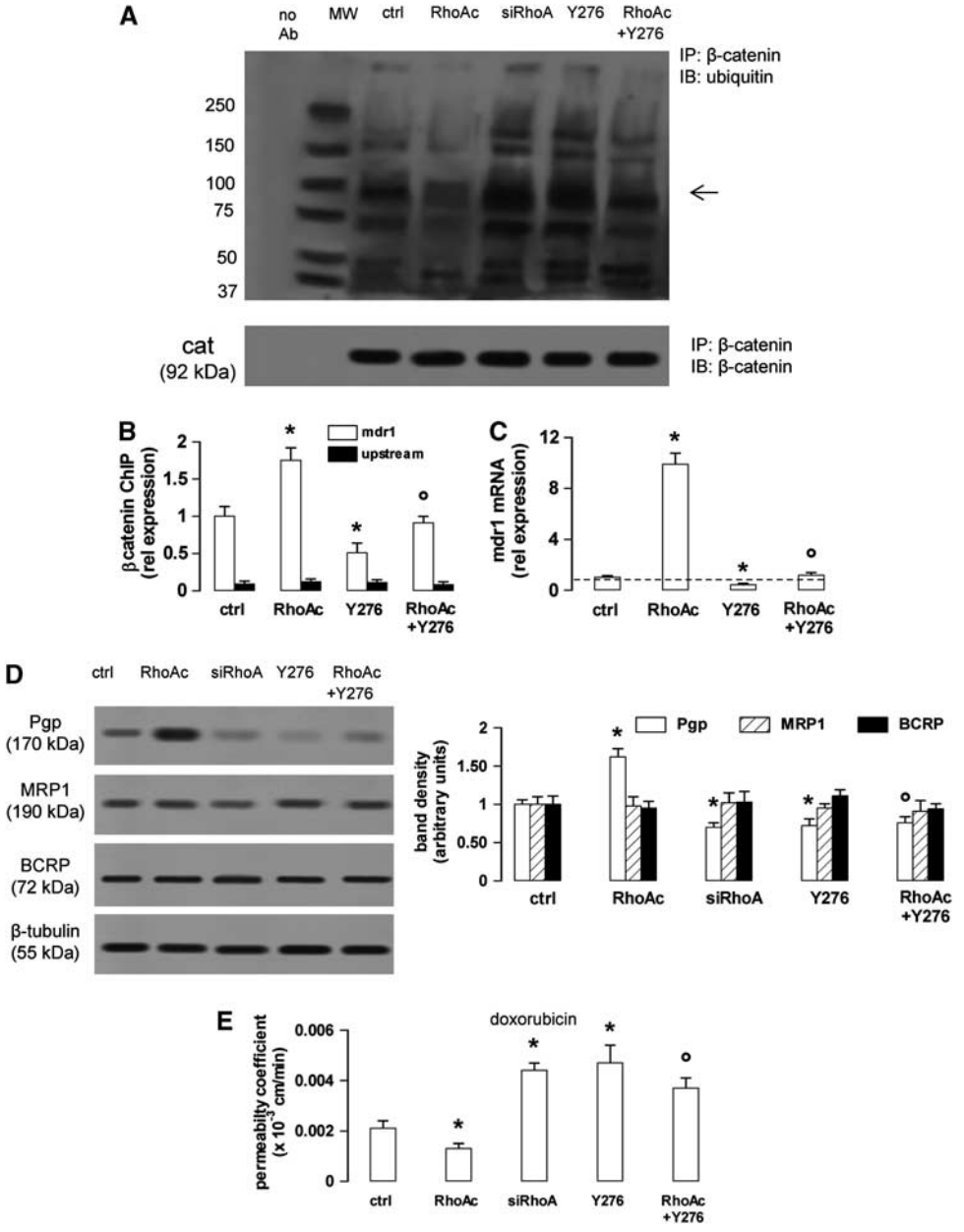

Figure 4. The RhoA kinase (RhoAK) inhibition enhances the ubiquitination of β-catenin, downregulates the β-catenin-induced transcription of P-glycoprotein (Pgp) and increases the doxorubicin permeability in human blood–brain barrier cells. The hCMEC/D3 cells were grown in fresh medium (ctrl), or in medium containing the RhoA activator II (RhoAc; 5 μg/mL for 3 hours) or the RhoAK inhibitor Y27632 (*Y276*; 10 μmol/L for 3 hours), alone or co-incubated. When indicated, the cells were treated with a non-targeting scrambled small interfering RNA (siRNA) or a RhoA-targeting specific siRNA (siRhoA) for 48 hours (panel **A**) or 72 hours (panels **D** and **E**). (**A**) Whole-cell lysates were immunoprecipitated (IP) with an anti-β-catenin antibody, then immunoblotted (IB) with an anti-mono/polyubiquitin antibody or with an anti-β-catenin antibody. Cells treated with non-targeting scrambled siRNA had the same level of ubiquitination than untreated (ctrl) cells (not shown). The figure is representative of three experiments with similar results. no Ab: samples immunoprecipitated without anti-β-catenin antibody. MW, molecular weight markers. The 92 kDa band corresponding to the native β-catenin protein is indicated by the arrow. (**B**) Chromatin immunoprecipitation assay. The genomic DNA was extracted, immunoprecipitated with an anti-β-catenin antibody and analyzed by qRT–PCR, using primers for the β-catenin-binding site on the mdr1 promoter (open bars) or for an upstream region (black bars), chosen as a negative control. Results are expressed as means ± s.d. ($n = 4$). Versus ctrl: $^*P < 0.05$; versus RhoAc: $^\circ P < 0.01$. (**C**) The mdr1 expression was detected by qRT–PCR. Data are presented as means ± s.d. ($n = 4$). Versus ctrl: $^*P < 0.005$; versus RhoAc: $^\circ P < 0.001$. (**D**) Western blot analysis of Pgp, multidrug resistance-related protein 1 (MRP1) and breast cancer resistance protein (BCRP) in the whole-cell lysates of hCMEC/D3 cells treated as described above. The β-tubulin expression was used as a control of equal protein loading. The figure is representative of three experiments with similar results. The band density ratio between each protein and β-tubulin was expressed as arbitrary units. Versus ctrl cells: $^*P < 0.02$; versus RhoAc: $^\circ P < 0.005$. (**E**) Doxorubicin permeability. The cells were grown for 7 days up to confluence in Transwell inserts and incubated as reported above. At the end of the incubation period, doxorubicin (5 μmol/L) was added in the upper chamber. After 3 hours the amount of drug recovered from the lower chamber was measured fluorimetrically. The permeability coefficient was calculated as reported under Materials and Methods. In cells treated with the non-targeting scrambled siRNA the permeability coefficient was 0.0018 ± 0.0002 (not significant versus ctrl cells). Measurements were performed in duplicate and data are presented as means ± s.d. ($n = 3$). Versus ctrl: $^*P < 0.05$; versus RhoAc: $^\circ P < 0.02$.

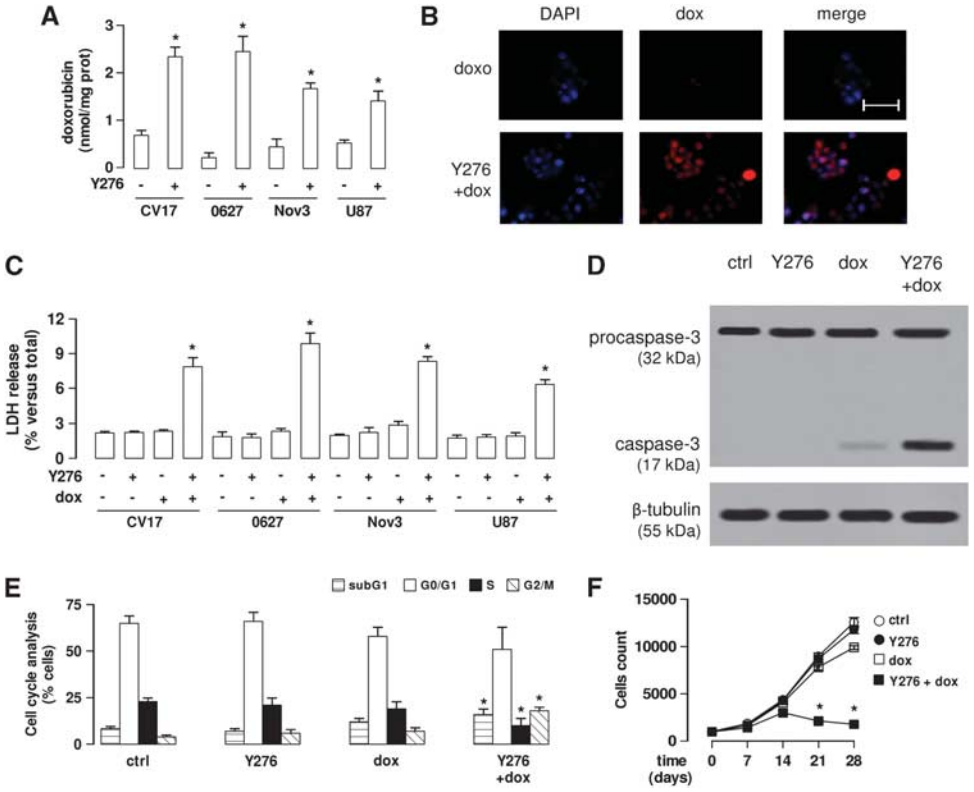

Figure 5. The RhoA kinase (RhoAK) inhibitor Y27632 increases the doxorubicin delivery and cytotoxicity in glioblastoma cells co-cultured with blood–brain barrier cells. The hCMEC/D3 cells were grown for 7 days up to confluence in Transwell inserts; CV17, 01010627, Nov3, and U87-MG cells were seeded at day 4 in the lower chamber. After 3 days of co-culture, the supernatant in the upper chamber was replaced with fresh medium without (− or ctrl) or with Y27632 (*Y276*; 10 μmol/L for 3 hours). After this incubation time, doxorubicin (dox; 5 μmol/L) was added in the upper chamber for 3 hours (panels **A** and **B**) or 24 hours (panels **C**–**F**), then the following investigations were performed. (**A**) Fluorimetric quantification of intracellular doxorubicin in glioblastoma cells. Data are presented as means ± s.d. ($n = 4$). Versus untreated (−) cells: $^*P < 0.001$. (**B**) The 01010627 cells were seeded on sterile glass coverslips, treated as reported above, then stained with 4′,6-diamidino-2-phenylindole dihydrochloride (DAPI) and analyzed by fluorescence microscopy to detect the intracellular accumulation of doxorubicin. Magnification: × 63 objective (1.4 numerical aperture); × 10 ocular lens. The micrographs are representative of three experiments with similar results. Scale bar, 20 μm. (**C**) The glioblastoma cells were checked spectrophotometrically for the extracellular release of lactate dehydrogenase (LDH) activity. Data are presented as means ± s.d. ($n = 4$). Versus untreated (−) cells: $^*P < 0.001$. (**D**) The whole-cell lysates from 01010627 cells were resolved by SDS–PAGE and immunoblotted with an anti-caspase 3 antibody (recognizing both pro-caspase and cleaved active caspase). The β-tubulin expression was used as a control of equal protein loading. The figure is representative of three experiments with similar results. (**E**) Cell cycle analysis. The distribution of the 01010627 cells in sub-G1, G0/G1, S, G2/M phase was analyzed by flow cytometry, as detailed under Materials and Methods. Data are presented as means ± s.d. ($n = 4$). Versus ctrl: $^*P < 0.005$. (**F**). After 3 days of co-culture between hCMEC/D3 and 01010627 cells, the medium of the upper chamber was replaced with fresh medium (open circles) or medium containing Y27632 (*Y276*; 10 μmol/L for 3 hours, solid circles), doxorubicin (dox; 5 μmol/L for 24 hours, open squares), Y27632 (*Y276*; 10 μmol/L for 3 hours) followed by doxorubicin (doxo; 5 μmol/L for 24 hours, solid squares). Drug treatments were repeated every 7 days, as reported in the Materials and Methods section. The proliferation of glioblastoma cells was monitored weekly by crystal violet staining. Measurements were performed in triplicate and data are presented as means ± s.d. ($n = 4$). Versus ctrl: $^*P < 0.001$.

It has not been clarified however whether the canonical Wnt pathway controls the activity of the non-canonical Wnt pathways or *vice versa*. In gastric cancer cells, the activation of RhoA in response to Wnt5a is dependent on the activation of the PI3K/Akt/GSK3 axis.[24] Our results demonstrated that an active RhoA decreases the activity of GSK3, prevents the GSK3-mediated phosphorylation of β-catenin, and favors its nuclear translocation and the subsequent transcription of Pgp, whereas the RhoA silencing produces opposite effects. We therefore hypothesize that the RhoA activity controls the GSK3/β-catenin axis in hCMEC/D3 cells. This hypothesis is in contrast with results obtained in murine cerebrovascular endothelial cells, where the activation of RhoA promotes the phosphorylation of β-catenin and reduces its transcriptional activity.[9] As murine and human brain microvascular cells have often striking differences in the expression and activity of Pgp,[25] it is not surprising that they also differ in the upstream pathways controlling Pgp expression. For instance, the mechanism by which RhoA modulates GSK3 activity is quite different in murine and human cerebrovascular endothelial cells: in murine cells, RhoA controls the GSK3 activity in a PTEN- and protein kinase Cδ-dependent way and changes the phosphorylation of GSK3 on serine 9.[9] This phosphorylation has inhibitory effects on the enzymatic activity of GSK3.[26] We cannot exclude that the RhoA activity may change the phosphorylation on serine 9 of GSK3 also in human hCMEC/D3 cells; however, we observed that in our model, the activation of RhoA decreases—and the silencing of RhoA increases—the phosphorylation of GSK3 on tyrosine 216, which is a proactivating phosphorylation.[26] When phosphorylated on tyrosine 216, GSK3 induces β-catenin phosphorylation and degradation. To our knowledge, this is the first work showing that RhoA activity modulates the phosphorylation on tyrosine 216 of GSK3.

We next looked for putative downstream effectors of RhoA responsible for this effect. We focused on RhoAK, whose activity followed the same trend of RhoA activity in response to WntA and Dkk-1 in hCMEC/D3 cells. Interestingly, the inhibition of RhoAK by Y27632 quickly decreased the nuclear translocation of β-catenin, with a maximal efficacy after 3 hours. At longer time points, nuclear β-catenin progressively re-accumulated in the nucleus, although it remained lower than in untreated cells: this may be due to the short half-life (i.e., less than 12 hours) of β-catenin,[27] which produces a fast re-synthesis of new β-catenin ready to translocate into the nucleus. After 3 hours, Y27632 effectively increased the phosphorylation on tyrosine 216 of GSK3 and the subsequent GSK3-induced phosphorylation of β-catenin; by acting downstream RhoA, Y27632 was effective even in cells with a constitutively activated RhoA. These data suggest that RhoAK likely controls the GSK3 activity by activating a tyrosine phosphatase, which recognizes GSK3 as substrate. PTP1B, which is activated by the phosphorylation on serine 50,[20] is one of these phosphatases.[19] Our results in hCMEC/D3 cells and in a cell-free system demonstrate that the RhoAK phosphorylates PTP1B on serine 50, promoting the dephosphorylation of GSK3 on tyrosine 216, an event that was fully abrogated by Y27632. These data suggest that the RhoAK, by activating PTP1B, inhibits the GSK3 activity, prevents the ubiquitination of β-catenin, and allows its nuclear translocation and transcriptional activity. Our results also explain previous observations, showing that Wnt3 stimulates the transcription of β-catenin-target genes and RhoA-target genes, with a putative RhoAK-dependent mechanism.[8]

Some β-catenin-target genes encode for proteins of adherens junctions and tight junctions; therefore, changes in RhoA/RhoAK activity may lead to the loss of BBB integrity.[10] In our experimental conditions, no changes occurred in the protein expression and functionality of tight junctions in the hCMEC/D3 cells treated with Y27632. By contrast, Y27632 was sufficient to reduce the β-catenin-driven transcription of Pgp. As different promoters have different sensitivity to the binding of β-catenin–T-cell factor complex, we might speculate that the promoter of Pgp is more sensitive than the promoter of other genes to the variations of β-catenin/T-cell factor binding.

Working at proper concentrations and incubation times, the RhoAK inhibitor increased the delivery of doxorubicin, a Pgp substrate with a very low permeability across the BBB.[13] Fasudil, the clinically prescribed analog of Y27632, is used to prevent vasospasms after subarachnoid hemorrhage,[28] to improve tissue perfusion during cerebral ischemia,[29] to prevent the progression of cerebral aneurisms.[30] Our work suggests that Fasudil might be used to improve the delivery of Pgp substrates through the BBB.

In the case of doxorubicin, a drug that is highly effective against glioblastoma cells *in vitro*[31] and ineffective in the presence of a competent BBB,[6] the pretreatment of hCMEC/D3 cells with Y27632 fully restored the doxorubicin delivery and cytotoxicity in glioblastoma cells. Repeated pulses of Y27632 followed by doxorubicin confirmed that this approach effectively reduced the long-term proliferation of glioblastoma cells grown under a BBB monolayer. However, Pgp is not the only transporter present on the luminal side of BBB that can efflux doxorubicin: also MRP1 and BCRP, which are detectable in the hCMEC/D3 cells,[11] meet these requisites,[1] but their expression did not change in cells with constitutively active RhoA, silenced for RhoA or treated with Y27632. We thus hypothesize that the changes in doxorubicin delivery after RhoA activation or inhibition were consequent to the expression change of Pgp in hCMEC/D3 cells. To further quantify the contribution of this transporter in doxorubicin permeability, we treated the hCMEC/D3 cells with the Pgp inhibitor verapamil, which produced the same effects—in terms of doxorubicin delivery and toxicity in glioblastoma cells—of Y27632. These results indirectly suggest that Pgp has a major role in limiting doxorubicin delivery in the central nervous system.

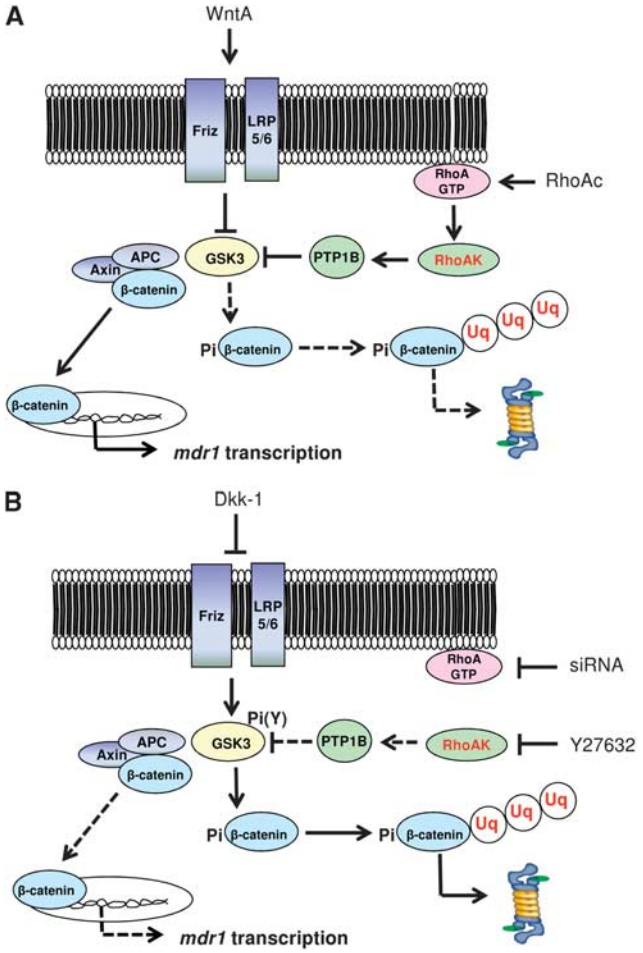

Figure 6. Cross-talk between Wnt/GSK3 pathway and Wnt/RhoA/RhoA kinase (RhoAK) pathway and effects on P-glycoprotein (Pgp) expression in human blood–brain barrier (BBB) cells. (**A**) The Wnt activators (WntA) reduce the glycogen synthase kinase 3 (GSK3)-mediated phosphorylation and ubiquitination of β-catenin, decreasing its proteasomal degradation. In these conditions, β-catenin is released from the APC/axin complex, translocates into the nucleus, and activates the transcription of mdr1 gene, which encodes for Pgp. The RhoA activation reduces as well the activity of GSK3: the active RhoA increases the activity of RhoAK, which induces the phosphorylation on serine 50 of protein tyrosine phosphatase 1B (PTP1B). After this phosphorylation, PTP1B dephosphorylates GSK3 on tyrosine 216 and inactivates it. Overall, the activation of the RhoA/RhoAK axis contributes to the transcription of β-catenin target genes, like mdr1. (**B**) The Wnt inhibitors (e.g., Dickkopf-1 (Dkk-1)) increase the GSK3-mediated phosphorylation and ubiquitination of β-catenin, priming it for the proteasomal degradation. The inhibition of RhoA (e.g., by RhoA small interfering RNA (siRNA)) or RhoAK (e.g., by Y27632) increases the GSK3 activity, by reducing the RhoAK-mediated phosphorylation of PTP1B on serine 50 and preventing the dephosphorylation of GSK3 on tyrosine 216. As a result, the nuclear translocation of β-catenin and its transcriptional activity are reduced, whereas the ubiquitination and proteasomal degradation of β-catenin are increased. These data lead to hypothesize the existence of a cross-talk between the Wnt/GSK3 canonical pathway and the Wnt/RhoA/RhoAK non-canonical pathway in human BBB cells. APC, adenomatous polyposis coli; Friz, Frizzled; LRP5/6, low density lipoprotein receptor-related protein 5/6; Pi, phosphate; Pi(Y), phosphotyrosine; RhoAc, RhoA activator II; RhoAK, RhoAK; Uq, ubiquitin. Continuous arrows indicate activated pathways; dotted arrows indicate inhibited pathways.

Although Pgp tightly cooperates with BCRP in controlling the delivery of several drugs across the BBB,[32] doxorubicin has high affinity for Pgp, which represents the main transporter of this drug in BBB cells.[33]

The downregulation of the canonical Wnt/GSK3/β-catenin pathway is known to reduce the Pgp expression and to induce chemosensitization in colon[34] and glioblastoma[17] tumor stem cells, neuroblastoma,[35] chronic myeloid leukemia,[36] and cholangiocarcinoma.[37] Also, the inhibition of the non-canonical Wnt3/RhoA/RhoAK pathway chemosensitizes multiple myeloma cells to doxorubicin.[38] We might speculate that the same cross-talk between canonical and non-canonical Wnt pathways, observed in BBB cells, cooperates in regulating the Pgp expression also in cancer cells, and may represent a critical target of therapeutic intervention for Pgp-rich tumors.

We suggest that the expression of Pgp is controlled by a cross-talk between canonical and non-canonical Wnt pathways in human BBB cells. A crucial regulator of this cross-talk is RhoAK, which inhibits the GSK3-induced phosphorylation of β-catenin by activating PTP1B. Targeted therapies against RhoA/RhoAK can disrupt the cross-talk and downregulate the Pgp expression (Figure 6). Improving the BBB permeability of anticancer drugs that are effluxed by Pgp thus enhancing their delivery to brain tumors is still an unsolved challenge.[39] Moreover, the high expression of Pgp on BBB cells decreases not only the delivery of chemotherapeutic agents, but also the passage of drugs used to treat infective diseases, neurodegenerative diseases, and epilepsy.[40] By unveiling a new mechanism that regulates Pgp expression in the BBB cells, our work may pave the way to preclinical investigations using RhoAK inhibitors as adjuvant tools in these central nervous system diseases.

DISCLOSURE/CONFLICT OF INTEREST

The authors declare no conflict of interest.

ACKNOWLEDGMENTS

The authors thank Mr Costanzo Costamagna, Department of Oncology, University of Turin for the technical assistance. We are grateful to Professor Davide Schiffer (Neuro-Biooncology Center, Vercelli, Italy) and Dr Rossella Galli (DIBIT, San Raffaele Scientific Institute, Milan, Italy) for providing the primary glioblastoma samples.

REFERENCES

1 Agarwal S, Sane R, Oberoi R, Ohlfest JR, Elmquist WF. Delivery of molecularly targeted therapy to malignant glioma, a disease of the whole brain. *Expert Rev Mol Med* 2011; **13**: e17.
2 Lim JC, Kania KD, Wijesuriya H, Chawla S, Sethi JK, Pulaski L *et al.* Activation of β-catenin signalling by GSK-3 inhibition increases p-glycoprotein expression in brain endothelial cells. *J Neurochem* 2008; **106**: 1855–1865.
3 Kania KD, Wijesuriya HC, Hladky SB, Barrand MA. Beta amyloid effects on expression of multidrug efflux transporters in brain endothelial cells. *Brain Res* 2011; **1418**: 1–11.
4 Katoh M, Katoh M. WNT signalling pathway and stem cells signaling network. *Clin Cancer Res* 2007; **13**: 4042–4045.
5 MacDonald BT, Tamai K, He X. Wnt/β-catenin signaling: components, mechanisms, and diseases. *Dev Cell* 2009; **17**: 9–26.
6 Riganti C, Salaroglio IC, Pinzòn-Daza ML, Caldera V, Campia I, Kopecka J *et al.* Temozolomide down-regulates P-glycoprotein in human blood-brain barrier cells by disrupting Wnt3-signalling. *Cell Mol Life Sci* 2014; **71**: 499–516.
7 Tsuji T, Ohta Y, Kanno Y, Hirose K, Ohashi K, Mizuno K. Involvement of p114-RhoGEF and Lfc in Wnt-3a- and dishevelled-induced RhoA activation and neurite retraction in N1E-115 mouse neuroblastoma cells. *Mol Biol Cell* 2010; **21**: 3590–3600.
8 Rossol-Allison J, Stemmle LN, Swenson-Fields KI, Kelly P, Fields PE, McCall SJ *et al.* Rho GTPase activity modulates Wnt3a/beta-catenin signaling. *Cell Signal* 2009; **21**: 1559–1568.
9 Chang CC, Lee PS, Chou Y, Hwang LL, Juan SH. Mediating effects of aryl-hydrocarbon receptor and RhoA in altering brain vascular integrity: the therapeutic potential of statins. *Am J Pathol* 2012; **181**: 211–221.
10 Allen C, Srivastava K, Bayraktutan U. Small GTPase RhoA and its effector rho kinase mediate oxygen glucose deprivation-evoked *in vitro* cerebral barrier dysfunction. *Stroke* 2010; **41**: 2056–2063.
11 Pinzón-Daza ML, Garzón R, Couraud PO, Romero IA, Weksler B, Ghigo D *et al.* The association of statins plus LDL receptor-targeted liposome-encapsulated doxorubicin increases the *in vitro* drug delivery across blood-brain barrier cells. *Brit J Pharmacol* 2012; **167**: 1431–1447.
12 Flatau G, Lemichez E, Gauthier M, Chardin P, Paris S, Fiorentini C *et al.* Toxin-induced activation of the G protein p21 Rho by deamidation of glutamine. *Nature* 1997; **387**: 729–733.
13 Weksler BB, Subileau EA, Perrière N, Charneau P, Holloway K, Leveque M *et al.* Blood-brain barrier-specific properties of a human adult brain endothelial cell line. *FASEB J* 2005; **19**: 1872–1894.
14 Doublier S, Riganti C, Voena C, Costamagna C, Aldieri E, Pescarmona G *et al.* RhoA silencing reverts the resistance to doxorubicin in human colon cancer cells. *Mol Cancer Res* 2008; **6**: 1607–1620.
15 Monnaert V, Betbeder D, Fenart L, Bricout H, Lenfant AM, Landry C *et al.* Effects of γ- and hydroxypropyl-γ-cyclodextrins on the transport of doxorubicin across an *in vitro* model of blood-brain barrier. *J Pharmacol Exp Ther* 2004; **311**: 1115–1120.
16 Eigenmann DE, Xue G, Kim KS, Moses AV, Hamburger M, Oufir M. Comparative study of four immortalized human brain capillary endothelial cell lines, hCMEC/D3, hBMEC, TY10, and BB19, and optimization of culture conditions, for an in vitro blood-brain barrier model for drug permeability studies. *Fluids Barriers CNS* 2013; **10**: e33.
17 Siflinger-Birnboim A, Del Vecchio PJ, Cooper JA, Blumenstock FA, Shepard JM, Malik AB. Molecular sieving characteristics of the cultured endothelial monolayer. *J Cell Physiol* 1987; **132**: 111–117.
18 Riganti C, Salaroglio IC, Caldera V, Campia I, Kopecka J, Mellai M *et al.* Temozolomide down-regulates P-glycoprotein expression in glioblastoma stem cells by interfering with the Wnt3a/GSK3/β-catenin pathway. *Neuro Oncol* 2013; **15**: 1502–1517.
19 Mobasher MA, González-Rodriguez A, Santamaría B, Ramos S, Martín MÁ, Goya L *et al.* Protein tyrosine phosphatase 1B modulates GSK3β/Nrf2 and IGFIR signaling pathways in acetaminophen-induced hepatotoxicity. *Cell Death Dis* 2003; **4**: e626.
20 Moeslein FM, Myers MP, Landreth GE. The CLK family kinases, CLK1 and CLK2, phosphorylate and activate the tyrosine phosphatase, PTP-1B. *J Biol Chem* 1999; **274**: 26697–26704.
21 Gottesman MM, Fojo T, Bates SE. Multidrug resistance in cancer: role of ATP-dependent transporters. *Nat Rev Cancer* 2002; **2**: 48–58.
22 Tai LM, Loughlin AJ, Male DK, Romero IA. P-glycoprotein and breast cancer resistance protein restrict apical-to-basolateral permeability of human brain endothelium to amyloid-β. *J Cereb Blood Flow Metab* 2009; **29**: 1079–1083.
23 de Jesus Perez VA, Alastalo TP, Wu JC, Axelrod JD, Cooke JP, Amieva M *et al.* Bone morphogenetic protein 2 induces pulmonary angiogenesis via Wnt-beta-catenin and Wnt-RhoA-Rac1 pathways. *J Cell Biol* 2009; **184**: 83–99.
24 Liu J, Zhang Y, Xu R, Du J, Hu Z, Yang L *et al.* PI3K/Akt-dependent phosphorylation of GSK3β and activation of RhoA regulate Wnt5a-induced gastric cancer cell migration. *Cell Signal* 2013; **25**: 447–456.
25 Uchida Y, Ohtsuki S, Katsukura Y, Ikeda C, Suzuki T, Kamiie J *et al.* Quantitative targeted absolute proteomics of human blood-brain barrier transporters and receptors. *J Neurochem* 2011; **117**: 333–345.
26 Jope RS, Johnson GV. The glamour and gloom of glycogen synthase kinase-3. *Trends Biochem Sci* 2004; **29**: 95–102.
27 Bareiss S, Kim K, Lu Q. Delta-catenin/NPRAP: A new member of the glycogen synthase kinase-3beta signaling complex that promotes beta-catenin turnover in neurons. *J Neurosci Res* 2010; **88**: 2350–2363.
28 Zoerle T, Ilodigwe DC, Wan H, Lakovic K, Sabri M, Ai J *et al.* Pharmacologic reduction of angiographic vasospasm in experimental subarachnoid hemorrhage: systematic review and meta-analysis. *J Cereb Blood Flow Metab* 2012; **32**: 1645–1658.
29 Shin HK, Huang PL, Ayata C. Rho-kinase inhibition improves ischemic perfusion deficit in hyperlipidemic mice. *J Cereb Blood Flow Metab* 2014; **34**: 284–287.
30 Eldawoody H, Shimizu H, Kimura N, Saito A, Nakayama T, Takahashi A *et al.* Fasudil, a Rho-kinase inhibitor, attenuates induction and progression of cerebral aneurysms: experimental study in rats using vascular corrosion casts. *Neurosci Lett* 2010; **470**: 76–80.
31 Hau P, Fabel K, Baumgart U, Rummele P, Grauer O, Bock A *et al.* Pegylated liposomal doxorubicin-efficacy in patients with recurrent high-grade glioma. *Cancer* 2004; **100**: 1199–1207.
32 Agarwal S, Hartz AM, Elmquist WF, Bauer B. Breast cancer resistance protein and P-glycoprotein in brain cancer: two gatekeepers team up. *Curr Pharm Des* 2011; **17**: 2793–2802.

33 Qu Q, Chu JW, Sharom FJ. Transition state P-glycoprotein binds drugs and modulators with unchanged affinity, suggesting a concerted transport mechanism. *Biochemistry* 2003; **42**: 1345–1353.
34 Chikazawa N, Tanaka H, Tasaka T, Nakamura M, Tanaka M, Onishi H *et al.* Inhibition of Wnt signaling pathway decreases chemotherapy-resistant side-population colon cancer cells. *Anticancer Res* 2010; **30**: 2041–2048.
35 Flahaut M, Meier R, Coulon A, Nardou KA, Niggli FK, Martinet D *et al.* The Wnt receptor FZD1 mediates chemoresistance in neuroblastoma through activation of the Wnt/beta-catenin pathway. *Oncogene* 2009; **28**: 2245–2256.
36 Corrêa S, Binato R, Du Rocher B, Castelo-Branco MT, Pizzatti L, Abdelhay E. Wnt/β-catenin pathway regulates ABCB1 transcription in chronic myeloid leukemia. *BMC Cancer* 2012; **12**: e303.
37 Shen DY, Zhang W, Zeng X, Liu CQ. Inhibition of Wnt/β-catenin signaling downregulates P-glycoprotein and reverses multi-drug resistance of cholangiocarcinoma. *Cancer Sci* 2013; **104**: 1303–1308.
38 Kobune M, Chiba H, Kato J, Kato K, Nakamura K, Kawano Y *et al.* Wnt3/RhoA/ROCK signaling pathway is involved in adhesion-mediated drug resistance of multiple myeloma in an autocrine mechanism. *Mol Cancer Ther* 2007; **6**: 1774–1784.
39 Serwer LP, James CD. Challenges in drug delivery to tumors of the central nervous system: an overview of pharmacological and surgical considerations. *Adv Drug Deliv Rev* 2012; **64**: 590–597.
40 Pinzón-Daza ML, Campia I, Kopecka J, Garzón R, Ghigo D, Riganti C. Nanoparticle- and liposome-carried drugs: new strategies for active targeting and drug delivery across blood-brain barrier. *Curr Drug Metab* 2013; **14**: 625–640.

Supplementary Information accompanies the paper on the Journal of Cerebral Blood Flow & Metabolism website (http://www.nature.com/jcbfm)